Proceedings of the ASME 2014 Dynamic Systems and Control Conference
DSCC2014
October 22-24, 2014, San Antonio, TX, USA

DSCC2014-6024

OBSERVER DESIGN FOR STATE ESTIMATION OF UV CURING PROCESSES

Adamu Yebi
Clemson University - International Center for Automotive Research
Greenville, SC 29607
ayebi@clemson.edu

Beshah Ayalew
Clemson University-International Center for Automotive Research
Greenville, SC 29607
beshah@clemson.edu

Satadru Dey
Clemson University - International Center for Automotive Research
Greenville, SC 29607
satadrd@clemson.edu

ABSTRACT

This article discusses the challenges of non-intrusive state measurement for the purposes of online monitoring and control of Ultraviolet (UV) curing processes. It then proposes a two-step observer design scheme involving the estimation of distributed temperature from boundary sensing cascaded with nonlinear cure state observers. For the temperature observer, backstepping techniques are applied to derive the observer partial differential equations along with the gain kernels. For subsequent cure state estimation, a nonlinear observer is derived along with analysis of its convergence characteristics. While illustrative simulation results are included for a composite laminate curing application, it is apparent that the approach can also be adopted for other UV processing applications in advanced manufacturing.

I. INTRODUCTION

Ultraviolet (UV) radiation curing of materials is a widely used process in photopolymerization of resins, coatings and adhesives. It is gaining substantial interest in other advanced manufacturing applications such as stereolithography and curing of composite laminates due to its several advantages such as 1) higher energy efficiency; 2) less environmental pollutions; 3) accelerated processing time; 4) reduced space usage and maintenance costs, and; 5) better controllability[1-3]. Despite these advantages, the thickness of parts that can be cured effectively by UV-radiation is limited because UV is attenuated as it passes through target materials according to the so-called Beer-Lambert effect [2]. As a result, extended irradiation may be needed to cure thick sections. However, in thick sections, the accompanying thermal and cure level gradients from the distributed exothermic cure reactions may compromise the quality and mechanical performance of the end product. This is often overcome by exhaustive offline optimization of process parameters such as exposure distance and intensity settings. For online monitoring and feedback process control, online adjustment of the radiative inputs is desirable but the distributed cure state information throughout the thickness of the section is rarely available in practice.

Most available cure level measurement options involve offline techniques that can be done on laboratory samples destructively. These include dynamic mechanical analyzer (DMA), rheometers and thermal differential scanning calorimeter (DSC) [4]. In some applications, there is the possibility of using online, albeit intrusive, measurements with non-reusable sensors (i.e. dielectric analyzer (DEA), fiber-optics, etc.) that are imbedded in the material to be cured and become part of the product at the end of curing. The latter are often expensive and may affect the quality of the end product as well[5]. In this paper, the design of state estimators/observers is considered as an economical, online, non-intrusive and nondestructive alternative to overcome the lack of suitable sensing options with these features for UV curing applications.

Manufacturing processes involving curing such as rapid prototyping, stereolithography[6] and layered composite manufacturing[7] involve exothermic chemical reactions activated by thermal or radiative energy sources. In these processes, the heat transfer in the part is modeled by a nonlinear partial differential equation (PDE) describing the spatio-temporal evolution of temperature in the part and the cure kinetics is often modeled by a nonlinear ordinary differential equation (ODE)[6, 7] describing the temporal evolution of the cure state. However, by virtue of the dependence of local reaction rates on local temperatures, the cure state is also spatially distributed and coupled to the temperature evolution. Despite this distribution of the temperature and cure states, the only non-intrusive practical measurements are often limited to boundary measurement of surface temperature via some optical sensors (IR thermal cameras). This limited sensing and the nature of the coupled nonlinear PDE-ODE models of the curing process make the estimator/observer design problems challenging.

The literature offers a number of nonlinear observer design methods that have been tested for various finite dimensional systems modeled by ODEs: for example, Lyapunov-based methods(Thau's[8] & Raghavan's[9]), geometric observer[10], and sliding mode observer[11]. Most of these are designed to guarantee convergence of state estimation errors under deterministic model assumptions. For nonlinear stochastic systems, extended Kalman filter (EKF)[12] and unscented Kalman filter (UKF)[13] are used dominantly, although the stated theoretical conditions for error convergence are often difficult to establish/verify. In the case of nonlinear infinite dimensional systems described by nonlinear PDEs, most of the observer designs extend the above methods by approximating the PDEs with representative ODEs. The common approximation techniques are finite difference methods [14], or Proper Orthogonal Decomposition (POD)-Galerkin methods[15]

While there appears to be limited prior work on observer designs specific to UV curing applications, some solutions have been proposed for related state estimation problems in similar applications. Soucy[16] used an extended Kalman filter to estimate the cure state in auto-clave curing of thick section composite laminates. The estimator construction assumed the online measurement of the distributed temperature state. For a similar problem, Parthasarathy, et al[14] introduced a nonlinear observer to estimate primarily the distributed temperature state. The cure state is subsequently computed using the open-loop cure kinetics model from the estimated temperature. In both of the above works, the estimator design was based on an approximated ODE version of the coupled PDE-ODE process model. Despite the ODE approximation error, the direct estimator of cure state in [16] is potentially more robust than the approach in [14] in the presence of disturbances and errors in guessing the initial state. However, the approach in [16] is useful only for a part thickness(depth) large enough to accommodate placement of a large number of temperature sensors across the thickness. This is impractical for UV curing, as there is a fundamental limitation on the thickness of parts that can be UV-cured due to the above-mentioned UV attenuation with depth.

A desirable observer for the UV curing application is an augmented or full-order observer of the coupled distributed temperature and cure state with the available boundary temperature measurement. However, the problem posed as such lacks observability as will be discussed in detail below. As a work around, in this paper, we design a two–step temperature and cure state observer. First, the infinite dimensional temperature observer is designed based on boundary PDE backstepping techniques[17] to generate a bounded estimate of the distributed temperature state. Then, this estimated temperature information is used to construct a nonlinear cure state observer with some guaranteed convergence conditions established via a Lyapunov analysis.

The remainder of the paper is organized as follows. Section II presents the problem statement considering a process model for UV curing a composite laminate. Section III discusses the observability of the problem and details the two-step observer designs. Section IV provides demonstrative simulation results. Section V gives the conclusions of the paper.

NOMENCLATURE

c_p : Specific heat of composite [$J/g\,^0C$]

E : Activation energy [J/mol]

h : Convective heat transfer [$W/cm^2\,^0C$]

I_0 : UV-light intensity at surface [W/cm^2]

k_z : Thermal conductivity of composite [$W/cm\,^0C$]

L : Cure level observer gain [-]

l : Sample thickness [cm]

$m \& n$: Reaction orders [-]

$p_1(x) \& p_{10}$: Temperature observer gains [-]

$p \& q$: Constants parameters [-]

R : Gas constant [$J/mol\,K$]

s : Photoinitiator concentration [$wt\%$]

$T(z,t)$: Temperature distribution in physical space [^0C]

T_{abs} : Absolute temperature [K]

T_∞ : Ambient temperature [^0C]

t : Time [$\sec$]

$w(x,t)$: Temperature in normalized space [^0C]

$\hat{w}(x,t)$: Temperature estimate in normalized space [^0C]

$\tilde{w}(x,t)$: Temperature estimation error [^0C]

x : Spatial direction for normalized space [-]

z : Spatial direction for physical space [cm]

$\alpha(z,t)$: Cure level distribution in physical space [%]

$\alpha_{\hat{w}}(x,t)$: Cure level for estimated temperature [%]

$\tilde{a}(x,t)$: Cure level estimation error [%]

ΔH_r : Polymerization enthalpy of resin [J/g]

ϑ : Absorptivity constant [-]

μ : Absorptivity of photoinitiator $[wt\% - cm]^{-1}$

v_r : Volumetric fraction of resin [-]

ρ : Density of composite [g/cm^3]

ρ_r : Density of resin [g/cm^3]

φ : Pre-exponential factor of rate constant [$\sec^{-1}$]

II. PROBLEM STATEMENT

We consider a 1D process for UV curing a fiberglass composite laminate. A schematic of the process set up is shown in Figure 1. The basis for the model is that of a UV curing process model verified for curing a pure unsaturated polyester resin for a stereolithography/photo-fabrication application [6]. The following three considerations are added to the basic model. First, a resin volume fraction factor is introduced in the process model to consider the fact that only the resin portion undergoes the photopolymerization reaction([7],[14]). Second, we take the average thermal properties of the resin and of the fiber for the properties of the composite laminate in the z-direction, which is the indicated direction of sample depth/thickness. Third, we model the attenuation of UV-radiation in the resin-fiber matrix in the z-direction according to Beer Lambert's Law, where a single attenuation constant will be taken for the laminate. This essentially assumes a uniformly wetted fiberglass and resin where the refractive indices of the fiber and resin are matched. To continue with this assumption for general cases, the attenuation constant for the combined resin-fiber matrix may need to be modified[18].

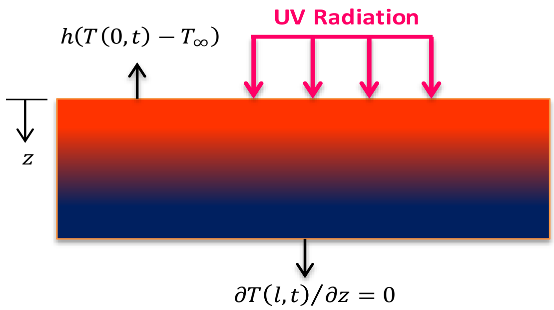

Fig. 1. Schematic of a UV Curing Process.

Considering the above considerations, the curing process model is given by the following coupled PDE-ODE systems along with the boundary conditions and initial conditions:

$$\begin{cases} \rho c_p \dfrac{\partial T(z,t)}{\partial t} = k_z \dfrac{\partial^2 T(z,t)}{\partial z^2} + v_r \Delta H_r \rho_r \dfrac{d\alpha(z,t)}{dt} & in\,\Omega_T \\ \dfrac{d\alpha(z,t)}{dt} = K(z,T)\alpha^m(z,t)\left(1-\alpha(z,t)\right)^n & in\,\Omega_T \\ K(z,T) = \varphi s^q I_0^p \exp\left(-E/RT_{abs}(z,t)\right)\exp(-\mu spz) & in\,\Omega_T \\ k_z \dfrac{\partial T(0,t)}{\partial z} + \vartheta * I_0(t) = h(T(0,t)-T_\infty) & in\,\Gamma_1 \\ \dfrac{\partial T(l,t)}{\partial z} = 0 & in\,\Gamma_2 \\ T(z,0) = T_0(z) & in\,\Omega \\ \alpha(z,0) = \alpha_0(z) & in\,\Omega \end{cases} \quad (1)$$

where ρ and c_p are the density and specific heat capacity of the composite laminate, respectively; k_z is the thermal conductivity of laminate in the z-direction; $T(z,t)$ is temperature distribution at depth z and time t; v_r is volumetric fraction of resin in the composite matrix; ρ_r is density of resin; and ΔH_r is polymerization enthalpy of resin conversion; E is activation energy, s is photoinitiator concentration φ is pre-exponential factor of rate constant; R is gas constant; I_0 is UV-light intensity; $T_{abs}(z,t)$ is absolute temperature in Kelvin; $\alpha(z,t)$ is cure level/state distribution; $m\&n$ are reaction orders; $p\&q$ are constant exponents; μ is the absorption coefficient of photoinitiator; ϑ is absorptivity constant of the UV-radiation at the boundary; h is convective heat transfer at the top boundary; l is the thickness of composite sample, and T_∞ is constant ambient temperature; and $d\alpha(z,t)/dt$ is the rate of cure conversion (rate of polymerization). The various domains and boundaries are: $\Omega_T \in [0,l]x[0,\infty)$, $\Omega \in [0,l]$, $\Gamma_1 \in \{0\}x[0,\infty)$, and $\Gamma_2 \in \{l\}x[0,\infty)$.

We simplify the process model (1) by introducing the following change of variables:

$$x = \frac{z}{l} \quad (2)$$

$$w(x,t) = T(x,t) - T_\infty \quad (3)$$

The simplified model is summarized in the following form:

$$\begin{cases} w_t(x,t) = \xi w_{xx}(x,t) + \gamma_a f(x,t,w,\alpha) & in\,\Omega_T \\ w_x(0,t) = \gamma_b w(0,t) - \lambda_b I_0 & in\,\Gamma_1 \\ w_x(1,t) = 0 & in\,\Gamma_2 \\ w(x,0) = w_0(x) & in\,\Omega \\ \dot{\alpha}(x,t) = f(x,t,w,\alpha) & in\,\Omega_T \\ \alpha(x,0) = \alpha_0(x) & in\,\Omega \end{cases} \quad (4)$$

The nonlinear term f represents the cure conversion rate and is given by:

$$f(x,t,w,\alpha) = \beta_a I_0^p \exp\left(\frac{-E}{R\left(w_{abs}(x,t)\right)}\right) * \alpha^m(x,t)\left(1-\alpha(x,t)\right)^n \exp(-\lambda_a x) \quad (5)$$

where $\xi = k_c/\rho c_p l^2$, $\gamma_a = v_r \rho_r \Delta H/\rho c_p$, $\lambda_a = p\mu sl$, $\beta_a = \varphi s^q$, $\gamma_b = hl/k_c$, $\lambda_b = \vartheta l/k_c$, $w_{abs}(x,t) = w(x,t) + T_\infty + 273$. The notation $\dot{\alpha}$, w_t, w_x, and w_{xx} represent $d\alpha/dt$, $\partial w/\partial t$, $\partial w/\partial x$ and $\partial^2 w/\partial x^2$, respectively.

Note that even though the above model has been discussed for a composite laminate, the essential process considerations are quite similar for other UV curing applications. One can directly use this model (by modifying the added considerations) and the discussions that follow for other UV curing applications in advanced manufacturing, such as photo-fabrication, 3D printing, curing coatings, etc.

III. PROPOSED OBSERVER STRUCTURE AND DESIGN

The primary objective of the observer is to estimate the distribution of cure state $\alpha(z,t)$ using the available boundary temperature measurement. On initial consideration, this objective might seem easily achievable by simply constructing a full state observer for both the temperature and cure level states. However, as will be shown in subsection A below, the full state is not observable using the adopted model with only boundary measurement of temperature.

To overcome this difficulty, we propose the two-step observer design shown schematically in Figure 2. First, a temperature observer is designed to generate a bounded estimate of the temperature distribution across the laminate. This estimated temperature distribution is then used in the cure state observer.

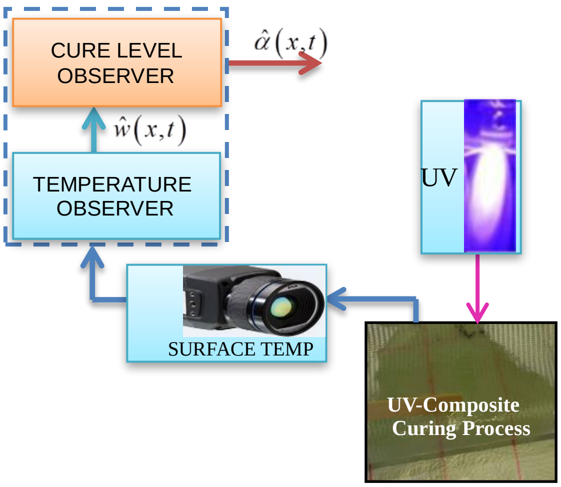

Figure2. Observer Design Structure

A. Observability Checks

For a linear system, observability is a global property for which there are well known criteria to check. For nonlinear systems such as the present application, the notion of observability depends on the regions of the state space where the system operates and as such it remains a local property. Several versions of local observability definitions and checks are available of which we apply the ones by Zeitz[19], also summarized in[20], to the present curing process model.

To check the observability of the full PDE-ODE system model for the curing process, we first derive an augmented nonlinear ODE system by applying central difference approximations for the spatial derivative in the PDE of (4). The resulting system dynamics and measurement equations can be written in the form:

$$\begin{cases} \dot{\chi}(t) = \bar{h}\left(\chi(t), u(t)\right),\ \chi(0) = \chi_0 \\ y(t) = \begin{bmatrix} 1 & 0 \end{bmatrix} \chi_1(t) \end{cases} \tag{6}$$

where $\chi = \begin{bmatrix} w \\ \alpha \end{bmatrix} = \chi = \left[\chi_1 \cdots \chi_{\bar{n}}\right]^T \in X$ is the augmented state vector of the temperature and cure state at each spatial discretization location, and $u = I_0^p \in U^0$ is a scalar UV input, χ_0 is the initial state vector and y is the boundary temperature measurement. $X \subset \mathbb{R}^{\bar{n}}$ and $U^0 \subset \mathbb{R}$ are connected open sets. $\bar{h}$ is a vector function of the spatially discretized state and input, and $\bar{n}$ is dimension of the augmented state χ, which is twice the size of the number of spatial discretization nodes adopted.

An ODE system of form (6) is said to be locally observable [20], if

$$rank\left\{ \frac{\partial}{\partial \chi} \begin{bmatrix} y \\ \frac{dy}{dt} \\ \vdots \\ \frac{d^{\bar{n}-1} y}{dt^{\bar{n}-1}} \end{bmatrix} \right\}_{(\chi^*, u^o)} = \bar{n} \tag{7}$$

$\forall \left(\chi^*, u^0, \cdots, u^{\bar{n}-1}\right) \in X \times U^0 \times \cdots \times U^{\bar{n}-1}$, where $u^b, b = 1, \cdots, \bar{n}-1$ is the b^{th} time derivative of u, and $\left(\chi^*, u^o\right)$ is nominal operating point.

Applying this test to the curing process model with a three-node discretization, (and, so a 6th order system: three for temperature and three for cure state), one finds that the observability matrix in (7) is of rank 3. It can be shown analytically that, for any discretization level, the rank is half the size of the full state space. So, the full state is not observable.

The two-part observer design is proposed to alleviate this difficulty.

B. Temperature Observer Design

With only boundary temperature sensing practically available for the UV curing process, we find that the backstepping boundary PDE observer design methods detailed in[17], among many others reviewed in [21], to be suitable for constructing the temperature observer. Since the backstepping design methods are developed primarily for linear PDEs, we exploit the observation that the present temperature PDE is a semi-linear PDE that is close to a linear one. Furthermore, since this PDE is coupled to the cure state dynamics, in order to proceed with the temperature observers design, we make the practical assumption that the rate of cure conversion $d\alpha(x,t)/dt$ is upper-bounded.

Using the backstepping approach, the temperature observer for process model (4) with surface (boundary) temperature sensing at the top $w(0,t)$ is constructed as follows:

$$\begin{cases} \hat{w}_t(x,t) = \xi \hat{w}_{xx}(x,t) + p_1(x)\left[w(0,t) - \hat{w}(0,t)\right] \\ \qquad + \gamma_a \hat{f}(x,t,\hat{w},\alpha_{\hat{w}}) & in\,\Omega_T \\ \hat{w}_x(0,t) = \gamma_b w(0,t) + p_{10}\left[w(0,t) - \hat{w}(0,t)\right] - \lambda_b I_0 & on\,\Gamma_1 \\ \hat{w}_x(1,t) = 0 & on\,\Gamma_2 \\ \hat{w}(x,0) = \hat{w}_0(x) & in\,\Omega \\ \dot{\alpha}_{\hat{w}}(x,t) = \hat{f}(x,t,\hat{w},\alpha_{\hat{w}}) & in\,\Omega_T \\ \alpha_{\hat{w}}(x,0) = \alpha_{\hat{w}0}(x) & in\,\Omega \end{cases} \tag{8}$$

where, $\hat{w}(x,t)$ is the estimated state of $w(x,t)$, $p_1(x)\,\&\,p_0$ are the observer gains, $\alpha_{\hat{w}}(x,t)$ is the cure state computed using the cure state ODE as an "open-loop" observer which uses the estimated temperature. The nonlinear term $\hat{f}$ represents the cure conversion rate in terms of estimated temperature and is given by:

$$\hat{f}(x,t,\hat{w},\alpha_{\hat{w}}) = \beta_a I_0^p \exp\left(\frac{-E}{R\left(\hat{w}_{abs}(x,t)\right)}\right) * \\ \alpha_{\hat{w}}^{\ m}(x,t)\left(1-\alpha_{\hat{w}}(x,t)\right)^n \exp(-\lambda_a x) \tag{9}$$

Defining the temperature observer error variable as $\tilde{w}(x,t) = w(x,t) - \hat{w}(x,t)$, and the cure state error $\tilde{\alpha}_{\hat{w}}(x,t) = \alpha(x,t) - \alpha_{\hat{w}}(x,t)$, and subtracting (8) from (4), the observer error dynamics becomes:

$$\begin{cases} \tilde{w}_t(x,t) = \xi \tilde{w}_{xx}(x,t) - p_1(x)\tilde{w}(0,t) + \tilde{f}(x,t,w,\hat{w},\alpha,\alpha_{\hat{w}}) & in\,\Omega_T \\ \tilde{w}_x(0,t) = -p_{10}\tilde{w}(0,t) & on\,\Gamma_1 \\ \tilde{w}_x(1,t) = 0 & on\,\Gamma_2 \\ \tilde{w}(x,0) = \tilde{w}_0(x) & in\,\Omega \\ \dot{\tilde{\alpha}}_{\hat{w}}(x,t) = \tilde{f}(x,t,w,\hat{w},\alpha,\alpha_{\hat{w}}) & in\,\Omega_T \\ \tilde{\alpha}_{\hat{w}}(x,0) = \tilde{\alpha}_{\hat{w}0}(x) & in\,\Omega \end{cases} \tag{10}$$

where, $\tilde{f}(x,t,w,\hat{w},\alpha,\alpha_{\hat{w}}) = \gamma_a\left(f(x,t,w,\alpha) - \hat{f}(x,t,\hat{w},\alpha_{\hat{w}})\right)$. Note that, the distributed temperature error dynamics in (10) consists of two parts: the first two terms constitute the linear part and the last term $\tilde{f}$ (cure conversion rate error) constitutes the nonlinear part.

Fact 1: Treating $\tilde{f}$ as unknown bounded disturbance, the observer designed to exponentially stabilize the linear part of the error dynamics PDE in (10) (ignoring $\tilde{f}$) leads to bounded temperature estimation error when applied to the full nonlinear PDE error dynamics (10) (including $\tilde{f}$). A proof is provided in Appendix A.

The design of the observer for the linear part of the PDE can be done following the approach detailed in [17]. The linear part of the of observer error dynamics (10) is given by:

$$\begin{cases} \tilde{w}_t(x,t) = \xi \tilde{w}_{xx}(x,t) - p_1(x)\tilde{w}(0,t) & in\,\Omega_T \\ \tilde{w}_x(0,t) = -p_{10}\tilde{w}(0,t) & on\,\Gamma_1 \\ \tilde{w}_x(1,t) = 0 & on\,\Gamma_2 \\ \tilde{w}(x,0) = \tilde{w}_0(x) & in\,\Omega \end{cases} \tag{11}$$

The observer gains $p_1(x)\,\&\,p_{10}$ can be determined by transforming the error system (11) to a stable target system (13) using the state transformation:

$$\tilde{w}(x,t) = v(x,t) - \int_0^x p(x,y)v(y,t)dy \tag{12}$$

The choice of particular stable target system is not unique but the following exponentially stable target system is considered convenient with tuning parameter $c > 0$:

$$\begin{cases} v_t(x,t) = \xi v_{xx}(x,t) - cv(x,t) & in\,\Omega_T \\ v_x(0,t) = 0 & on\,\Gamma_1 \\ v_x(1,t) = 0 & on\,\Gamma_2 \\ v(x,0) = v_0(x) & in\,\Omega \end{cases} \tag{13}$$

The proof for the exponential stability of a similar target system as (13) is provided in our previous work[22] and also in [23].

We use the transformation in (12) along with (11), to derive the following conditions for the observer gain kernel $p(x,y)$ and observer gains:

$$p_{xx}(x,y) - p_{yy}(x,y) = -\frac{c}{\xi}p(x,y) \tag{14}$$

$$p_x(1,y) = 0 \tag{15}$$

$$p(x,x) = \frac{c}{2\xi}(x-1) \tag{16}$$

The observer gains are:

$$p_1(x) = \xi p_y(x,0) \tag{17}$$

$$p_{10} = p(0,0) \tag{18}$$

Solving (14-16) analytically, the observer gain kernel and ultimately the gains can be shown to be:

$$p(x,y) = -\frac{c}{\xi}(1-y)\frac{I_1\left(\sqrt{\frac{c}{\xi}(2-x-y)(x-y)}\right)}{\sqrt{\frac{c}{\xi}(2-x-y)(x-y)}} \tag{19}$$

$$p_1(x) = c\left(\frac{I_1\left(\sqrt{\frac{c}{\xi}x(2-x)}\right)}{\sqrt{\frac{c}{\xi}x(2-x)}} + \frac{I_2\left(\sqrt{\frac{c}{\xi}x(2-x)}\right)}{x(2-x)}\right) \tag{20}$$

$$p_{10} = -\frac{c}{2\xi} \tag{21}$$

Using these gains in the temperature observer PDE (8) along with the "open-loop" cure state estimates, we can generate the distributed temperature estimate, with bounded estimation errors via Fact 1.

C. *Cure State Observer Design*

For brevity of notations, we drop the independent variables t and x in the cure state dynamics and we rewrite it as follows:

$$\dot{\alpha} = f(w,\alpha) \tag{22}$$

Before we proceed, note that (22) is to be spatially discretized along the same discretization as adopted for implementing the temperature observer PDE (8). Therefore, with some abuse of notation, α is the cure state vector indexed by spatial location $x \in [0, 1/\bar{p}, \cdots, 1]^T$ where $\bar{p}$ is the number of discretization points, and therefore, the size of the cure state vector. The function $f(w,\alpha)$, which represents the cure conversion rate, can be factored into nonlinear functions of input and state as follows:

$$f(w,\alpha) = r(w)g(\alpha) \tag{23}$$

where $r(w) = \beta_a I_0^p \exp(-E/R(w_{abs}))\exp(-\lambda_a x)$, and $g(\alpha) = \alpha^m(1-\alpha)^n$.

For strongly nonlinear systems like those of the cure dynamics (22), a common estimation approach is the extended Kalman filter (EKF) [24, 25]. However, the computational cost of recursively computing the gains is high and verifying the sufficient conditions for stability is not trivial. To overcome these deficiencies, we propose a variable structure cure state observer design where Lyapunov analysis is used to establish theoretical convergence conditions and then process specific modifications are applied for implementation.

Assuming that the estimated temperature from the temperature observer is sufficiently accurate (by the observer design), we proceed with the cure state observer design by treating $\hat{w} \approx w$. The cure state observer is then constructed using the process dynamics (22) and supposing that a pseudo-measurement signal $y = \dot{\alpha}$ can be obtained by inverting the temperature estimate obtained via (8). Under these considerations, the pseudo-measurement signal can also be written as:

$$y = f(\hat{w},\alpha) \tag{24}$$

Given (22) and (24), we can construct the observer as follows:

$$\dot{\hat{\alpha}} = f(\hat{w},\hat{\alpha}) + L\left(y - \dot{\hat{\alpha}}\right) \tag{25}$$

where the cure state estimate is denoted by $\hat{\alpha}$ and the observer gain L is a diagonal $\bar{p} \times \bar{p}$ matrix.

We introduce the following change of variables[20] to later avoid the need for computing the time derivative $\dot{w}$ in the pseudo-measurement (inversion of (8)),

$$\hat{\alpha} = Z + L/\gamma_a \hat{w} \tag{26}$$

Substituting (26) into (25), we reconstruct the observer (24) in the following implementable form:

$$\dot{Z} = f\left(\hat{w},(Z + L/\gamma_a \hat{w})\right)[1-L] - \frac{L}{\gamma_a}\left(\xi \hat{w}_{xx} + p_1 \tilde{w}(0)\right) - \frac{\dot{L}}{\gamma_a}\hat{w} \tag{27}$$

For stability analysis we re-write the observer dynamics in the form:

$$\dot{\hat{\alpha}} = f(\hat{w},\hat{\alpha}) + L\left(f(\hat{w},\alpha) - f(\hat{w},\hat{\alpha})\right) \tag{28}$$

Introducing the estimation error variable $\tilde{\alpha} = \alpha - \hat{\alpha}$, subtracting (28) from (22), and substituting (23) the error dynamics takes the form:

$$\dot{\tilde{\alpha}} = (1-L)\tilde{g}(\alpha,\hat{\alpha})r(\hat{w}) \tag{29}$$

where $\tilde{g}(\alpha,\hat{\alpha}) = g(\alpha) - g(\hat{\alpha})$.

Since the elements in the cure state vector are decoupled from each other, we can design the diagonal observer gain elements separately by using an element-wise Lyapunov function candidate

$$V_i = \frac{1}{2}\tilde{\alpha}_i^2,\ i = 1,...,\bar{p} \tag{30}$$

Taking the time derivative of Lyapunov function (30) and substituting the element-wise error dynamics (29),

$$\dot{V}_i = (1-L_i)\tilde{g}_i(\alpha,\hat{\alpha})\tilde{\alpha}_i r_i(\hat{w}) \tag{31}$$

where, $r(\hat{w}) > 0, \forall \hat{w}$. It is clear that to make $\dot{V}_i < 0$ (stable observer), the gains L_i have to switch sign based on the sign of $\tilde{g}_i(\alpha,\hat{\alpha})\tilde{\alpha}_i$. The latter is not readily pre-determined. We apply the following process specific considerations to overcome this limitation of the observer design.

Remark: I. Figure (3) shows the evolution of $g(\alpha)$ as a function of the cure state. The maximum of $g(\alpha)$ occurs at $\alpha = m/[m+n]$, which is explicitly dependent only on the reaction order constants m and n. The function $g(\alpha)$ is strictly increasing function of α until $g(\alpha)$ reaches its peak value. Then after, it becomes a decreasing function of α.

Since $\hat{\alpha}$ is computed/available, it can be determined that $g(\hat{\alpha})$ lies in the first zone if $\hat{\alpha} \le m/[m+n]$ and it lies in the second zone if $\hat{\alpha} > m/[m+n]$. An estimate of $g(\alpha)$ can be computed from the pseudo-measurement (24) (i.e. $g(\alpha) = y/r(w)$ assuming $\hat{w} \approx w$). Then, the gradient ($dg(\alpha)/dt$) can be computed, and combined with the observation that the cure rate $y \ge 0, \forall t$, one can determine that $g(\alpha)$ lies in the first zone if $dg(\alpha)/dt \ge 0$, and the second zone if $dg(\alpha)/dt < 0$.

To choose the observer gains, we consider two cases:

Case 1: If $g(\alpha)$ and $g(\hat{\alpha})$ are in the same zone: $\tilde{a}_i\tilde{g}_i(a,\hat{a}) \geq 0$ in the first zone, and $\tilde{a}_i\tilde{g}_i(a,\hat{a}) \leq 0$ in the second zone. Therefore, to make $\dot{V}_i \leq 0$, in the first zone we chose $L_i > 1$, and in the second zone we chose $L_i < 1$.

Case 2: If $g(\alpha)$ and $g(\hat{\alpha})$ are in different zones: the sign $\tilde{a}_i\tilde{g}_i(a,\hat{a})$ cannot be predetermined; still the sign of L_i can be chosen as a sign of $\tilde{a}_i\tilde{g}_i(a,\hat{a})$ based on the knowledge of the magnitudes of $g(\alpha)$ and $g(\hat{\alpha})$.

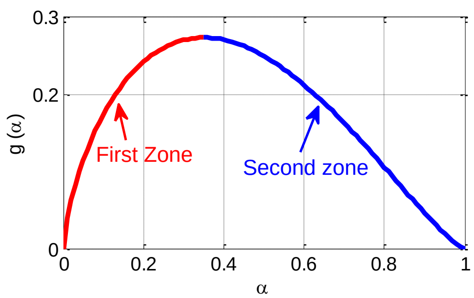

Figure 3: Evolution of Function $g(\alpha)$ with Cure State α

Remark II. In practice, the process starts from uncured state. One can choose initial cure state estimates near zero, and it is possible to have convergence of the estimate using a constant gain in the first zone. For the second zone, the observer gain can be switched to zero where the observer becomes open-loop stable. However, the latter removes a means of tuning the observer.

Remark III. In the implementable form of the observer given in (27) there is an $\dot{L}$ term. While switching the observer gain, this term may produce unacceptable spikes. To avoid this, one can simply place saturation on this term (or replace the sign function with some smooth approximation).

IV. RESULTS AND DISCUSSIONS

In this section, we present simulation results to demonstrate the performance of the proposed two-step observer. The simulation considers the 1D UV curing model (4) as the process model. The associated thermal, chemical and material constants for photopolymerization of unsaturated polyester resin are extracted from published work[6, 26]. For the fiberglass, E-glass thermal properties such as thermal conductivity, ($k = 0.012 W/cm.^oC$), specific heat ($c_p = 0.8 J/g.^oC$), and density ($\rho = 2.55 g/cm^3$) are used. Volume fractions of 40% and 60% are used for fiber and resin, respectively to determine the average thermal properties of the composite laminate. A thickness of 5 mm is considered for the composite laminate. A constant UV-intensity of 60 mW/cm^2 is used for the entire curing duration, which is as long as 500 seconds.

For solving the PDEs, a forward in time and central in space (FTCS) finite difference method was used for both the process model and the temperature observer. A coarse grid of 11 nodes and a fine grid of 21 nodes were considered for the observer and process models, respectively. In both respective models, the same level of discretization was used for both the cure state and temperature state.

The decay rate of the temperature observer error can be tuned with the free parameters imbedded in the observer gains of (20) and (21). For the cure state observer, the practical case in remark II is considered with a constant gain element greater than one for all cure state elements in the first zone and then switched to zero gain (open-loop observer) in the second zone.

The performance of the observer is illustrated in two ways. Figure 4 shows the spatial distribution and the evolution of the spatial 2-norm of the observation error for temperature state plotted on a faster time scale. The observation error for cure state is plotted similarly in Fig.5.

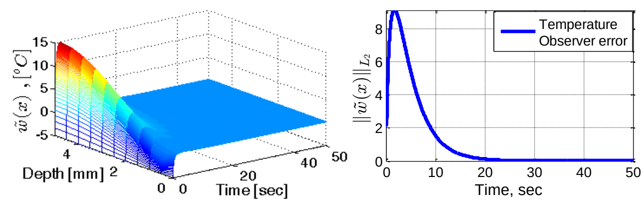

Fig.4: Convergence of Observer Error for Temperature State: (a) Spatial Distribution, and (b) Spatial 2-norm

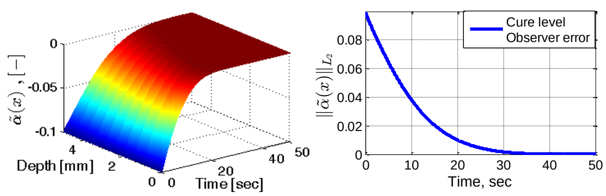

Fig.5: Convergence of Observation Error for Cure State: (a) Spatial Distribution, and (b) Spatial 2-norm

The results in Figs. 4 and 5 show that the initial temperature and cure state errors quickly stabilize in about 20 and 30 seconds, respectively. It should be recalled that since the cure state observer uses the output injection term from the temperature observer, the performance of the cure state observer is dependent on the performance of the temperature observer. This can be verified by close examination of Figs.4a &5a. For the backstepping temperature observer with observer gain (p_{10}) at top surface boundary in addition to in domain gain ($p_1(x)$), the temperature errors near the top boundary converge faster than those near the bottom boundary. The cure level observer error also follows the same trend since it uses the estimated temperature.

The performance of proposed two-step observer is also tested in the presence of measurement noise by adding a white, zero mean Gaussian noise on the boundary measurement. For a candidate boundary temperature sensor (IR-camera) with precision of $\pm 2^oC$, we assumed the Gaussian noise to have a covariance of this magnitude. Figures 6 & 7 show results for representative nodal points: top ($z=0$), middle ($z=0.5l$) and bottom ($z=l$), respectively. In this case, we considered a reduced cure level observer gain to show the error convergence after significant cure evolution is achieved. The error convergence is achieved in the first zone as it is stated in remark II.

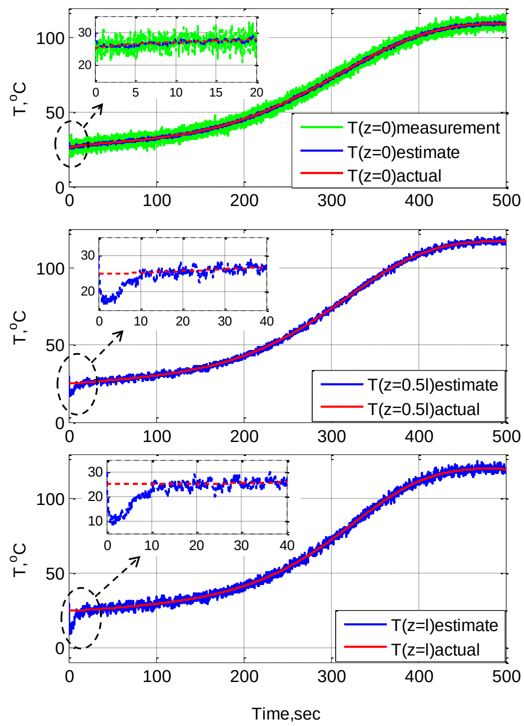

Figure 6: Evolution of Actual and Estimate Temperature at the Top, Middle and Bottom Nodes along the Depth of the Laminate.

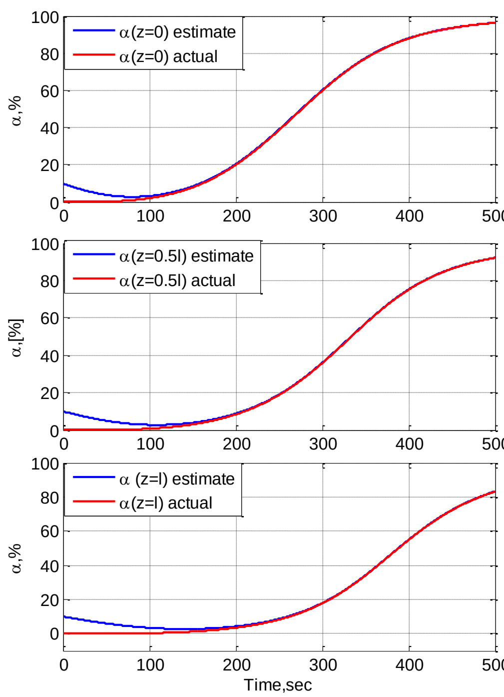

Figure 7: Evolution of Actual and Estimate Cure level at the Top, Middle and Bottom Nodes along the Depth of the Laminate

The results in Fig. 6 show that the estimate of temperature converges to the actual state in a short time. However, the influence of noise in the measurement is more pronounced as we go from top to bottom. This is as a result of observer gain (19) increasing in magnitude in the same direction. This variation of observer gain along depth is shown in Fig. 8. Also, the result in Fig.7 shows the convergence of cure state. It can be seen that the noise in the temperature measurement is not transmitted to the cure-state estimate. This is because of the negligible effect of noise in the temperature as it enters the cure dynamics in the exponential form $\exp\left(-E/R\hat{w}_{abs}\right)$. In the cure state observer, the noise in Z and $\left(L/\gamma_a\right)\hat{w}$ cancel each other while computing the cure level estimate via (26).

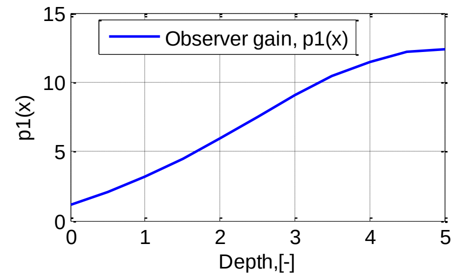

Figure 8: Variation of Observer Gain $p_1(x)$ with Depth

V. CONCLUSIONS

This paper proposed an online estimation scheme for obtaining cure state information in radiative UV curing processes. Considering the challenge of observability from practically available boundary temperature measurement, the paper outlined a two-step observer as a cascade of a distributed temperature observer and a nonlinear cure state observer. Assuming bounds on the nonlinear contribution of cure conversion on the temperature dynamics, backstepping PDE observer design techniques are applied to derive a distributed temperature observer. For cure state estimation, a variable structure nonlinear observer is designed assuming an accurate temperature estimate from the previous step. The performance of the proposed observer was tested through simulations of a process model for UV curing of a fiberglass composite laminate. The results showed that the proposed two-step observer performs well even in the presence of measurement noise.

ACKNOWLEDGMENTS

This research has been supported, in part, by the National Science Foundation under grant no. CMMI-1055254 and the US Department of Energy's GATE Program.

REFERENCES

[1] I. F. P. Roose, C. Vandermiers, M.-G. Olivier & M. Poelman, "Radiation curing technology: An attractive technology for metal coating," *Progress in Organic Coatings* vol. 64, p. 8, 2009.

[2] M. F. Perry and G. W. Young, "A mathematical model for photopolymerization from a stationary laser light

source," *Macromolecular theory and simulations,* vol. 14, pp. 26-39, 2005 2005.
[3] P. Compston, J. Schiemer, and A. Cvetanovska, "Mechanical properties and styrene emission levels of a UV-cured glass-fibre/vinylester composite," *Composite Structures,* vol. 86, pp. 22-26, 2008 2008.
[4] R. Schwalm, *UV Coatings: Basics, Recent Developments and New Applications*: Elsevier, 2006.
[5] J.-Y. C. a. S.V.Hoa, "Fiber-Optic and Ultrasonic measurements for In-situ Cure Monitoring of Graphite/Epoxy Composite," *Journal of Composite materials,* vol. 33, p. 22, 1999.
[6] J. M. Matias, P. J. Bartolo, and A. V. Pontes, "Modeling and simulation of photofabrication processes using unsaturated polyester resins," *Journal of Applied Polymer Science,* vol. 114, pp. 3673-3685, 2009 2009.
[7] X. Wang, "Modeling of in-situ laser curing of thermoset-matrix composites in filament winding," PhD Dissertation, university of Nebraska, 2001.
[8] F. E. Thau, "Observing the State of Nonlinear Dynamical Systems," *International journal of control* vol. 17, 1973.
[9] S. Raghavan and J. K. Hedrick, "Observer design for a class of nonlinear systems," *International Journal of Control,* vol. 59, pp. 515-528, 1994 1994.
[10] A. J. Krener and W. Respondek, "Nonlinear observers with linearizable error dynamics," *SIAM Journal on Control and Optimization,* vol. 23, pp. 197-216, 1985 1985.
[11] S. V. Drakunov, "An adaptive quasioptimal filter with discontinuous parameters," *Avtomatika i Telemekhanika,* pp. 76-86, 1983 1983.
[12] H. W. Sorenson, *Kalman filtering: theory and application* vol. 38: IEEE press New York, 1985.
[13] S. J. Julier and J. K. Uhlmann, "A new extension of the Kalman filter to nonlinear systems," 1997, pp. 3-2.
[14] S. Parthasarathy, S. C. Mantell, and K. A. Stelson, "Estimation, control and optimization of curing in thick-sectioned composite parts," *Journal of dynamic systems, measurement, and control,* vol. 126, pp. 824-833, 2004 2004.
[15] J. Baker and P. D. Christofides, "Finite-dimensional approximation and control of non-linear parabolic PDE systems," *International Journal of Control,* vol. 73, pp. 439-456, 2000 2000.
[16] K. A. Soucy, "Process modeling, state estimation, and feedback control of polymer composite processing," Washington Univ., Seattle, WA (United States)1991 1991.
[17] M. Krstic and A. Smyshlyaev, *Boundary control of PDEs: A course on backstepping designs* vol. 16: Society for Industrial Mathematics, 2008.
[18] A. Endruweit, W. Ruijter, M. S. Johnson, and A. C. Long, "Transmission of ultraviolet light through reinforcement fabrics and its effect on ultraviolet curing of composite laminates," *Polymer Composites,* vol. 29, pp. 818-829, 2008 2008.
[19] M. Zeitz, "The Extended Luenberger Observer for Nonlinear Systems," *Systems & Control Letters,* vol. 149, 1987.
[20] M. Soroush, "Nonlinear state-observer design with application to reactors," *Chemical Engineering Science,* vol. 52, pp. 387-404, 1997 1997.
[21] Z. Hidayat, R. Babuska, B. De Schutter, and A. Nunez, "Observers for linear distributed-parameter systems: A survey," 2011, pp. 166-171.
[22] A. Yebi and B. Ayalew, "Feedback Compensation of the In-Domain Attenuation of Inputs in Diffusion Processes," in *American Control Conference (ACC)*, Washington, DC, USA, 2013, pp. 2092 - 2097.
[23] A. Smyshlyaev and M. Krstic, *Adaptive control of parabolic PDEs*: Princeton University Press, 2010.
[24] K. Reif, S. Günther, E. Yaz Sr, and R. Unbehauen, "Stochastic stability of the discrete-time extended Kalman filter," *IEEE Transactions on Automatic Control,* vol. 44, pp. 714-728, 1999 1999.
[25] K. Reif, F. Sonnemann, and R. Unbehauen, "An EKF-based nonlinear observer with a prescribed degree of stability," *Automatica*, vol. 34, pp. 1119-1123, 1998 1998.
[26] P. Bártolo, "Optical approaches to macroscopic and microscopic engineering," University of Reading, 2001.

APPENDIX A

PROOF FOR TEMPERATURE OBSERVER

In this section, a brief proof is provided for Fact 1. Starting with a Lyapunov function candidate:

$$V(t) = \frac{1}{2}\int_0^1 \tilde{w}^2(x,t)dx \tag{A1}$$

Taking the derivative of (A1), applying PDE &BCs in (10), and integrating by parts:

$$\dot{V}(t) = \xi p_{10}\tilde{w}^2(0,t) - \xi\int_0^1 \tilde{w}_x^2(x,t)dx - \int_0^1 p_1(x)\tilde{w}(0,t)\tilde{w}(x,t)dx + \int_0^1 \tilde{f}(x,t,w,\hat{w},\alpha,\alpha_{\hat{w}})\tilde{w}(x,t)dx \tag{A2}$$

Assuming an upper bound on $\left\|\tilde{f}(x,t,w,\hat{w},\alpha,\alpha_{\hat{w}})\right\| \le \left|\tilde{F}(x)\right|$, we have

$$\dot{V}(t) \leq \xi p_{10}\tilde{w}^2(0,t) - \xi \int_0^1 \tilde{w}_x^2(x,t)dx - \int_0^1 p_1(x)\,\tilde{w}(0,t)\tilde{w}(x,t)dx + \int_0^1 \left|\tilde{F}(x)\right|\tilde{w}(x,t)dx \qquad \text{(A3)}$$

Equation (A3) can be re-written by substituting (20) and (21) in A(3)

$$\dot{V}(t) \leq \underbrace{-\frac{c}{2}\tilde{w}^2(0,t) - \xi \int_0^1 \tilde{w}_x^2(x,t)dx - c\int_0^1 N(x)\,\tilde{w}(0,t)\tilde{w}(x,t)dx}_{Linear\ part} + \underbrace{\int_0^1 \left|\tilde{F}(x)\right|\tilde{w}(x,t)dx}_{Nonlinear\ part} \qquad \text{(A4)}$$

where $N(x) = \dfrac{I_1\left(\sqrt{\frac{c}{\xi}x(2-x)}\right)}{\sqrt{\frac{c}{\xi}x(2-x)}} + \dfrac{I_2\left(\sqrt{\frac{c}{\xi}x(2-x)}\right)}{x(2-x)} \geq 0,\ for\ x \in [0,1]$.

For the selected exponential stable target system (12), the linear part in (A4) can be made negative with proper selection of design parameters c leading to the exponential convergence of the linear part of the PDE(9) [17]. However, due to the nonlinear part in (A4), the estimation error may not converge to zero. However, the Lyapunov derivative $\dot{V}$ will be negative until the following condition is satisfied:

$$\left|-\frac{c}{2}\tilde{w}^2(0,t) - \xi \int_0^1 \tilde{w}_x^2(x,t)dx - c\int_0^1 N(x)\,\tilde{w}(0,t)\tilde{w}(x,t)dx\right| > \left|\int_0^1 \left|\tilde{F}(x)\right|\tilde{w}(x,t)dx\right|$$

This essentially means that the estimation error will reach to a certain bounded manifold and will subsequently stay there. The manifold size is determined by the selection of design parameters c and size of the bound on the nonlinear term $\left|\tilde{F}(x)\right|$ With selection of high values of c, the steady-state estimation error can be made sufficiently small.